

Lattice dynamics of hexagonal MoS₂ studied by neutron scattering*

N. Wakabayashi, H. G. Smith, and R. M. Nicklow

Solid State Division, Oak Ridge National Laboratory, Oak Ridge, Tennessee 37830

(Received 10 February 1975)

Phonon-dispersion curves for the hexagonal-layered compound MoS₂ have been measured at room temperature by inelastic-neutron-scattering techniques for the [100] and [001] directions. The results have been analyzed on the basis of a model which includes valence forces between atoms in a layer and axially symmetric forces between atoms in neighboring layers. While the model reproduces the essential over-all features of the data, the present analysis indicates the need for a more sophisticated treatment of valence forces and/or for the inclusion of the atomic polarizabilities. The temperature dependence of the specific heat and the Debye temperature have been calculated from the model.

I. INTRODUCTION

The electronic properties of transition-metal dichalcogenides¹ with layer-type crystal structures have been investigated extensively in recent years. These compounds range from insulators to metals and their properties have been found to show marked anisotropy, with electrical conductivities within the layers being two orders of magnitude larger than those perpendicular to the layers. Very few studies have been reported of their vibrational properties, which are also expected to exhibit anisotropy. Wieting and Verble² made infrared and Raman measurements of lattice vibrations in MoS₂ and found that interactions between the neighboring layers are extremely small compared to those between atoms within a layer.

In this paper, we present phonon dispersion curves for the semiconductor MoS₂, obtained experimentally by neutron-inelastic-scattering techniques.

II. VIBRATIONAL MODES IN LAYERED COMPOUNDS

In MoS₂ a layer consists of one plane of Mo atoms sandwiched by two planes of sulfur atoms. In hexagonal MoS₂, which belongs to the space group D_{6h}^4 , two of these layers build the repeating unit in the c direction so that the unit cell contains six atoms, two of Mo and four of S. The basic structure of bonding within a layer is illustrated in Fig. 1. The a and c lattice parameters are 3.15 and 12.3 Å, respectively. Since there are six atoms per unit cell, in general there are 18 branches of the phonon dispersion relation, but in high-symmetry directions of the reciprocal space some branches are degenerate.

It is convenient to classify the various branches in terms of their group-theoretical representations. In the [001] direction there are four irreducible representations, Δ_1 , Δ_2 , Δ_5 , and Δ_6 .³ Δ_1 and Δ_2 are nondegenerate and each of them contains three branches which are purely longitudinal. Δ_5 and Δ_6 are doubly degenerate and six branches which are

purely transverse belong to each of these representations. There are also four irreducible representations in the [100] direction, Σ_1 , Σ_2 , Σ_3 , and Σ_4 , all of which are nondegenerate. There are six Σ_1 's, six Σ_3 's, two Σ_2 's, and four Σ_4 's. Σ_2 and Σ_4 are purely transverse modes with polarization vectors parallel to the basal plane, and in the modes belonging to Σ_2 , Mo atoms are stationary with S atoms within a layer moving in opposite directions. Σ_1 and Σ_3 are neither purely longitudinal nor purely transverse. In Σ_1 motions of Mo atoms have only components parallel to the basal plane, whereas in Σ_3 , they have only components perpendicular to the plane. Although these modes are of mixed character, the acoustic modes may be regarded to be either mostly longitudinal (Σ_1) or mostly transverse (Σ_3), and may be designated as LA, TA₁, or

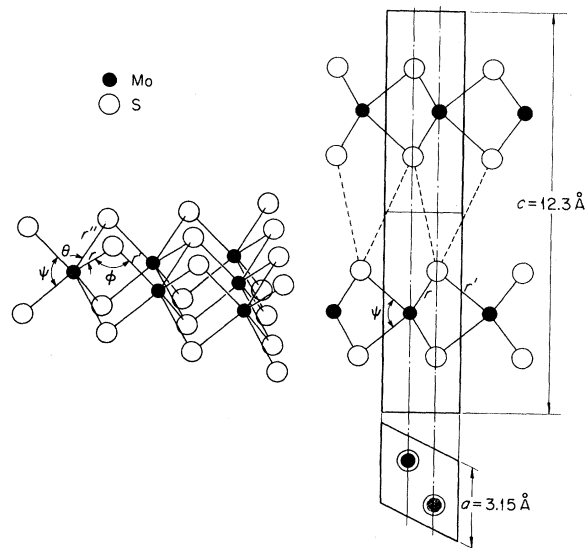


FIG. 1. Left drawing is to show the structure of bonding within a layer of hexagonal MoS₂. Right drawing shows the relative configuration of neighboring layers. The basal projection of the atomic positions is shown below. The unit cell is outlined by heavy lines.

Δ_{\perp} , where \perp (\parallel) signifies that the eigenvectors are perpendicular (parallel) to the basal plane. Vibrational modes at the Γ point have been discussed in detail by Wieting and Verble.²

Anisotropy in the various physical properties is closely related to the quasi-two-dimensional character of the crystal structure. The layers are so loosely bound that the interlayer interactions may be treated as small perturbations on isolated layers. Consequently, except along the c direction, each phonon branch may be considered to be paired to another branch which has nearly the same frequency. Such a pair would be a doubly degenerate branch if there were no interactions between the layers. For wave vectors along the c direction certain modes correspond to displacements of each layer as a rigid unit. The frequencies of these so-called rigid-layer modes are extremely low since they are determined mainly by the weak interlayer interactions.

III. EXPERIMENTAL RESULTS

The measurements were performed with a triple-axis neutron spectrometer located at the High Flux Isotope Reactor of ORNL. The MoS_2 crystal is a 2-mm-thick rectangular plate with the surface area of about $13 \times 8 \text{ cm}^2$. The mosaic spread of the sample about the c axis was estimated to be approximately 1° and the c axis is perpendicular to the surface of the sample. The crystal was mounted on the sample holder so that the c axis was in the scattering plane. Since the dimension of the incident neutron beam was $5 \times 3.5 \text{ cm}^2$, only part of the sample was irradiated.

All the measurements were carried out in the constant- \bar{Q} mode of operation. Because of the large c -lattice parameter, combined with the rather large mosaic spread of the sample, it was very difficult to obtain scans without some type of neutron beam (such as second- and third-order effects) contamination, and it was necessary to use various scattered-neutron energies ranging from 4 to 10 THz to sort out false peaks due to these effects.

Measurements were made along the $[001]$ and the $[100]$ directions, and the results are shown in Fig. 2. The uncertainties in the frequencies are in general about 5% except for those shown specifically in the figure. Since the Σ_2 and Σ_4 modes have polarization vectors perpendicular to the scattering plane, they were not observed in the present experiment. Except for the region of very low frequencies ($< 2 \text{ THz}$), all the branches are expected to be nearly degenerate in pairs, as discussed in Sec. II. It was not possible to observe each branch separately, and the data shown do not permit a distinction to be made between the two branches of each pair.

A few measurements of the low-frequency

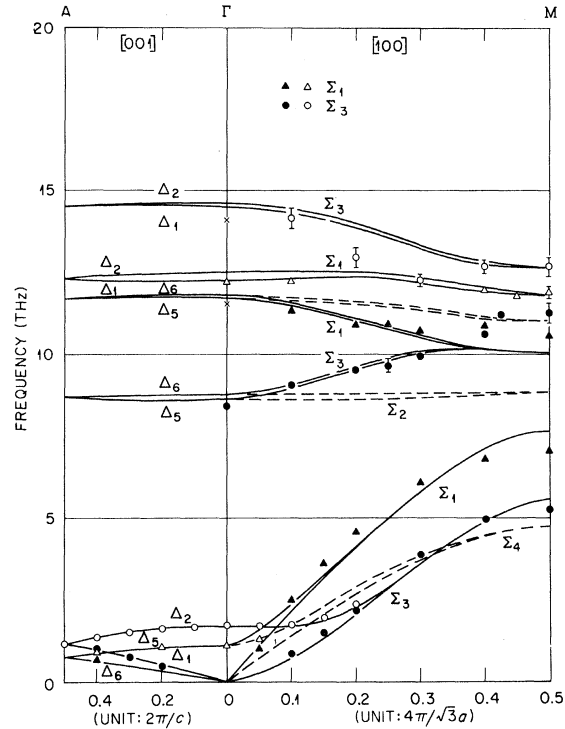


FIG. 2. Phonon dispersion curves for hexagonal MoS_2 along the $[001]$ and $[100]$ directions. Σ_2 and Σ_4 branches cannot be observed due to the geometrical restriction of the shape of the sample crystal. The lines are the calculated curves based on the model described in the text.

branches were made along the $[110]$ direction; it was found that the frequency of a phonon with a wave vector q less than $0.3(4\pi/a)$ is almost identical to that of a phonon in the $[100]$ direction that has a wave vector with the same magnitude. This isotropy of the phonon dispersion curves in the basal-plane directions was also found in the case of pyrolytic graphite.⁴ Some of the frequencies of the phonons at Γ could not be determined owing to the low neutron scattering intensities, but those observed are in good agreement with the results of the optical measurements by Wieting and Verble.² The very-low-frequency branches in the $[001]$ direction are those corresponding to the rigid-layer modes which are determined mainly by the interlayer forces.

Experimental data for the transverse-acoustic mode (ΣTA_1) in the $[100]$ direction seem to indicate a very small initial slope for that branch, as one might expect from the symmetry of a hexagonal structure. The initial slope of this branch is required by symmetry (rotational invariance) to be equal to that of the transverse-acoustic mode in the $[001]$ direction (ΔTA).⁵ In fact, if there were no interlayer interactions, the frequencies for the ΔTA would be identically zero and the ΣTA_1 branch

would have a dispersion curve of quadratic form in q near Γ .

IV. ANALYSIS

One of the simplest models that may be used to describe the lattice dynamics of a crystal is the axially symmetric model⁶ which assumes that the interatomic interactions are given by superpositions of central potentials. This assumption may be justified in the present case for the interlayer interaction, which for MoS₂ is considered to arise from weak van der Waals forces. However, in view of the strong covalent character of the intralayer interactions, a valence-force model⁷ should provide a more suitable description of these interactions. Therefore in the present analysis a mixed model has been used: The interlayer interaction is assumed to be due to an axially symmetric force between sulfur atoms of neighboring layers, and the intralayer interactions are assumed to be associated with the stretching and bending of Mo-S bonds. The bonds and bond angles considered in the model are shown in Fig. 1. In terms of the force constants K_r , K_θ , K_ϕ , and K_ψ , the potential energy is written as

$$\frac{1}{2} K_r (\Delta r)^2 + \frac{1}{2} K_\theta (r_0 \Delta \theta)^2 + \frac{1}{2} K_\phi (r_0 \Delta \phi)^2 + \frac{1}{2} K_\psi (r_0 \Delta \psi)^2,$$

where r_0 is the bond length. In addition there should be the cross terms that represent the interference between the changes in the lengths of different bonds, for example, $K_{rr'}^\theta (\Delta r) (\Delta r')$ and $K_{rr'}^\phi (\Delta r) (\Delta r')$, or between the stretching and the bending of a bond, for example, $K_{r\theta} (\Delta r) (r_0 \Delta \theta)$ and $K_{r\phi} (\Delta r) (r_0 \Delta \phi)$. There are also two parameters, α and β , corresponding to central forces between the sulfur atoms on different layers. These force constants are defined as

$$\alpha = \left. \frac{d^2 V}{dr^2} \right|_{r=R} \quad \text{and} \quad \beta = \left. \frac{1}{r} \frac{dV}{dr} \right|_{r=R},$$

where V is the interatomic potential and R is the equilibrium distance between the sulfur atoms of neighboring layers.

TABLE I. Force constants determined for MoS₂ from analysis of dispersion-curve measurements. Units: 10^5 dyn/cm.

K_r	1.3846
K_θ	0.1502
K_ϕ	0.1892
K_ψ	0.1381
$K_{rr'}^\theta$	-0.1722
α	0.0311
β	0.0072

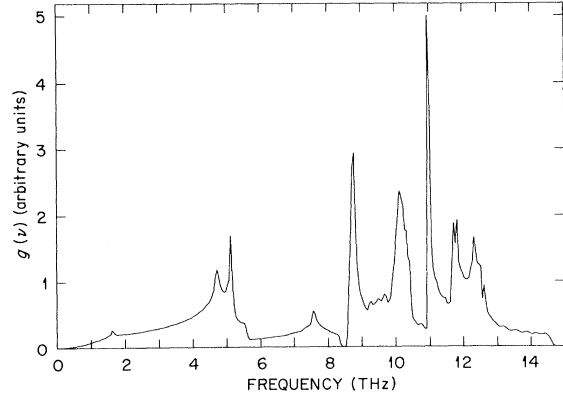


FIG. 3. Phonon density of states $g(\nu)$ calculated from the model.

The result of a least-squares fit of the data to a model which includes the six parameters α , β , K_r , K_θ , K_ϕ , and K_ψ was found to be inadequate to reproduce the data for large wave vectors. Since sulfur atoms are situated at low-symmetry positions, one might expect a large contribution to the potential function from the cross term due to $K_{rr'}^\phi$. A fit to a model that includes this additional parameter was in significantly better agreement with the data. Force constants determined by the fit are given in Table I, and the dispersion curves calculated from this model are shown in Fig. 2. In the Σ direction, solid lines represent the Σ_1 and Σ_3 branches and the broken lines the Σ_2 and Σ_4 branches, which were not observed experimentally. The restriction on the force constants imposed by the rotational invariance is not satisfied, and the elastic constant C_{44} calculated from ΔTA and ΣTA_1 differs almost by a factor of 2. Including one more parameter, $K_{rr'}^\theta$, in the model did not improve the quality of the fit, and, in fact, $K_{rr'}^\theta$ thus determined had a value smaller than that of $K_{rr'}^\phi$, by about an order of magnitude. Therefore, the seven-parameter model was used to calculate the phonon density of states $g(\nu)$ and the temperature dependence of the specific heat.

The frequency distribution $g(\nu)$ was calculated by the Raubenheimer-Gilat⁹ method adapted for the present model. The result is shown in Fig. 3. The peaks near 8.8 and 11.0 THz seem to be due to very flat branches, as one can see, for example, from the calculated dispersion curves for the Σ_2 and Σ_4 modes. Since these modes were not observed in the present experiment, those prominent peaks may be quite model dependent. However, the over-all features should be accurate enough to give a fairly reliable calculation of the temperature dependence of the specific heat. As shown in Fig. 4, the calculated specific heat has the T^3 dependence only below 6 K, similar to that of graphite.⁴ From this result, the temperature dependence of the

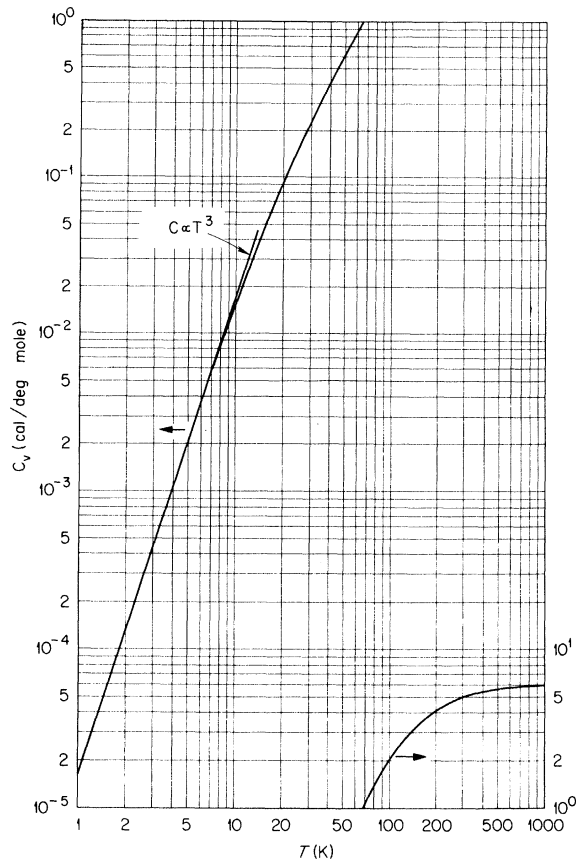


FIG. 4. Specific heat C_v calculated from the density of states shown in Fig. 3.

Debye temperature has been derived and is shown in Fig. 5. An interesting point is that the Debye temperature is a monotonically increasing function of temperature in the region above 1 K, for which the calculation was carried out, and the high-temperature Θ_D is almost twice as large as that of zero temperature. This behavior seems to be common to those materials that have large c -lattice constants and extremely weak interlayer interactions.

V. DISCUSSION

Although the present model seems to reproduce the essential features of the experimental results, there are, for large values of the wave vector, discrepancies clearly outside of the experimental uncertainties. In order to investigate the possible effects of the polarizabilities of the atoms, a very simple shell model⁹ in which only Mo atoms were assumed to be polarizable was constructed. Although the sulfur atoms are probably more polarizable, the calculations of the Coulomb interactions are very simple in the present model, and this model permits an estimate of the possible influence

of the polarizability on the phonon dispersion curves. It was found that if the polarizability was made large enough to affect the frequencies for large \vec{q} 's, the splitting between the longitudinal- and transverse-optic modes became too large to be consistent with the results of the optical measurements.² Also, the relevant Coulomb coefficients for wave vectors in the c direction were found to be smaller than those in the a - b plane by more than three orders of magnitude. This is due to the extremely large c/a ratio of the crystal, and the electrostatic interactions, therefore, will not appreciably affect the dispersion curves in the [001] direction. In order to improve the model, it is probably necessary to include the polarizability of sulfur, and/or the covalent character of the bonding must be treated more accurately by including additional cross terms in the potential function. In the present analysis, the choice of the most significant cross term was made rather arbitrarily. The only reasonable criterion would come from the detailed knowledge of the electronic configuration of the bonding between the molybdenum and sulfur atoms, and various efforts in recent years^{10,11} may eventually produce accurate information about the electronic wave functions of the ground and excited states in this and similar materials.

MoS₂ is not a superconductor, but some of the layered compounds are superconductors with high transition temperatures ($T_C = 6-7$ K for NbSe₂). Although mechanisms for superconductivity other than that of BCS have been proposed for those compounds, it is now generally accepted that the electron-phonon mechanism is mainly responsible, and it would be of considerable interest to search for indications of strong electron-phonon interactions in these compounds. An attempt to do so has been carried out for NbSe₂.¹² However, because of the small size of a single crystal available to us (< 0.05 cm³), only limited information about the

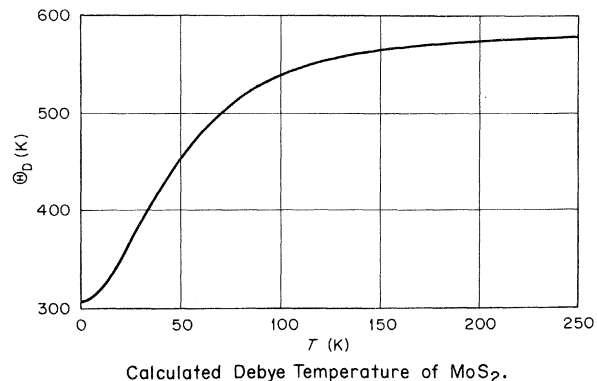


FIG. 5. Temperature dependence of the Debye temperature calculated from the C_v shown in Fig. 4.

phonon dispersion curves could be obtained. There is an indication of the existence of anomalies in the

dispersion curves which may be related to the two-dimensional Kohn anomaly.

*Research sponsored by the Energy Research and Development Administration for Union Carbide Corp.

¹J. A. Wilson and A. D. Yoffe, *Adv. Phys.* **18**, 193 (1969).

²T. J. Wieting and J. L. Verble, *Phys. Rev. B* **3**, 4286 (1971).

³Group-theoretical notations are those in J. C. Slater, *Quantum Theory of Molecules and Solids* (McGraw-Hill, New York, 1965), Vol. 2.

⁴R. M. Nicklow, N. Wakabayashi, and H. G. Smith, *Phys. Rev. B* **5**, 4951 (1972).

⁵For example, F. I. Fedorov, *Theory of Elastic Waves in Crystals* (Plenum, New York, 1968).

⁶G. W. Lehman, T. Wolfram, and R. E. DeWames, *Phys. Rev.* **128**, 1593 (1962).

⁷H. L. McMurry, A. W. Solbrig, Jr., and J. K. Boyter, *J. Phys. Chem. Solids* **28**, 2359 (1967).

⁸L. J. Raubenheimer and G. Gilat, *Phys. Rev.* **157**, 586 (1967).

⁹W. Cochran, *CRC Crit. Rev. Solid State Sci.* **2**, 1 (1971).

¹⁰G. Lucovsky and R. M. White, *Phys. Rev. B* **8**, 660 (1973).

¹¹L. F. Mattheiss, *Phys. Rev. B* **8**, 3719 (1973).

¹²N. Wakabayashi, H. G. Smith, and H. R. Shanks, *Phys. Lett. A* **50**, 367 (1974).